# Changes of Extreme Events in Regional Climate Simulations over East Asia

P4 A

Gao Xuejie (高学杰)① and Zhao Zongci (赵宗慈)

*National Climate Center, Beijing, 100081*

Filippo Giorgi

*Abdus Salam International Centre for Theoretical Physics, Trieste, Italy*

(Received September 22, 2001; revised August 1, 2002)

ABSTRACT

Changes of extreme events due to greenhouse effects ($2 \times CO_2$) over East Asia, with a focus on the China region as simulated by a regional climate model (RegCM2), are investigated. The model is nested to a global coupled ocean–atmosphere model (CSIRO R21L9 AOGCM). Analysis of the control run of the regional model indicates that it can reproduce well the extreme events in China. Statistically significant changes of the events are analyzed. Results show that both daily maximum and daily minimum temperature increase in $2 \times CO_2$ conditions, while the diurnal temperature range decreases. The number of hot spell days increases while the number of cold spell days decreases. The number of rainy days and heavy rain days increases over some sub-regions of China. The $2 \times CO_2$ conditions also cause some changes in the tropical storms affecting China.

**Key words:** regional climate model, greenhouse effect, extreme events

## 1. Introduction

Extreme climatic events can have profound impacts on natural ecosystems and a range of human activities. Indeed, one of the aspects that has recently drawn increasing attention within the global change debate is the assessment of impacts of possible changes in the frequency and intensity of extreme weather and climate events (e.g., Mearns et al. 2001). Analysis of simulated future changes in extreme events under enhanced forcing by greenhouse gases has been carried out within the context of both global model simulations and regional climate model (RCM) simulations (e.g., Mearns et al. 1999; Schar et al. 1996; Frei et al. 1998; Hennessy et al. 1997; Durman et al. 2001). These studies have indicated a general trend of increasing frequency of daily high temperature extremes, decrease in the frequency of daily minimum temperature extremes, increase in both the intensity of precipitation events and the frequency of extreme precipitation events, and increase in the occurrence of droughts or dry spells (Giorgi et al. 2001).

Impacts of climatic extremes are very important for the China region. Tropical storms, floods, and droughts have in fact caused enormous human and economic loss in China. For example, devastating floods occurred in 1991, 1996, 1998, and 1999 along the Yangtze River Valley and sustained droughts occurred in 1997, 1999, and 2000 over North China. During

①E-mail: gaoxj@cma.gov.cn

the last 50 years, an average of 7 typhoon landings over China have been observed, with the number varying from 3 to 12 for individual years (12 typhoon landings over China occurred for example in 1971 and 1994). Temperature extremes over China have also received much attention. For example, the warmest winters in the observational record over the region have taken place since 1986 and the number of days with temperature in excess of 36°C over different areas of North China has steadily increased during the 1990s. Similarly, hot spells have shown a steady increase in recent decades. Thus, it is important to assess the possible changes in the frequency and intensity of extreme events over China as anthropogenic activities continue to increase the global concentration of radiative forcing agents such as greenhouse gases (GHG) and atmospheric aerosols.

In this paper, we present a nested Regional Climate Model (RCM) study of changes in different measures of extreme temperature and precipitation events over East Asia due to increasing GHG concentration. Use of RCMs can be especially useful for the simulation of extreme events due to the relatively high horizontal resolution of these models, which allows a more realistic description of synoptic scale weather systems. We analyse two nested GCM / RCM multi-year simulations, one for present-day climate conditions, and another for conditions at a doubling of GHG concentration extracted from a transient climate change simulation. Results are analysed for simulated maximum and minimum daily temperature, number of rainy days, and number of heavy rain days. Changes in simulated tropical storms affecting the China region are also examined.

We first present a brief description of the model and experiment design in section 2. The results from the simulations are then analysed in section 3 and summary considerations are presented in section 4.

## 2. Model description and experiment design

The regional climate model used in the present work is the RegCM developed by Giorgi et al. (1993a, b) with some of the developments discussed in Giorgi and Shields (1999) and Giorgi et al. (1999). The dynamical core of the RegCM is essentially equivalent to the hydrostatic version of the NCAR / Pennsylvania State University mesoscale model MM5. Surface processes are represented via the Biosphere–Atmosphere Transfer Scheme (Dickinson et al. 1993) and boundary layer physics is formulated following the non-local scheme of Holtslag et al. (1990). Resolvable scale precipitation is represented via the simplified explicit scheme described by Giorgi and Marinucci (1996) and Giorgi and Shields (1999), which includes a prognostic equation for cloud water content, while the mass flux scheme of Grell (1993) is used to describe convective precipitation. Finally, radiative transfer is described using the radiation package of the NCAR Community Climate Model, version CCM3 (Kiehl et al. 1996), which describes the effect of different greenhouse gases ($CO_2$, $CH_4$, $N_2O$, CFCs), cloud ice effects, and atmospheric aerosols. Cloud radiation is calculated in terms of cloud fraction and cloud water content and the fraction of cloud ice is diagnosed by the scheme as a function of temperature.

The RegCM is driven by lateral boundary conditions provided by the Commonwealth Scientific and Industrial Research Organization (CSIRO) coupled Atmosphere–Ocean General Circulation Model (AOGCM) (Gordon and O'Farrell 1997). The atmospheric component of the CSIRO AOGCM has a horizontal spectral resolution of R21, corresponding to approximately $5.6° \times 3.2°$ longitude–latitude grid point spacing. The CSIRO AOGCM was integrated for the period 1881–2100 using observed GHG forcing until 1990 and a 1% per

year GHG concentration increase between 1990 and 2100, with no inclusion of sulfate aerosol effects. This simulation is described in detail by Gordon and O'Farrell (1997). Out of this 220–year simulation period, the two 5–year periods of 1986–1990 and 2066–2070 (corresponding to a doubling of GHG concentration compared to 1990) were selected for RegCM nesting to represent present–day (Control) and future ($2\times CO_2$) climate conditions, respectively. The nesting procedure utilizes a standard relaxation method as described, for example, by Giorgi et al. (1993b). Note that the RegCM has already been run with boundary conditions provided by the CSIRO model by Giorgi and Shields (1998) over the continental U.S., showing generally good performance in simulating temperature and precipitation climatology over that region.

The domain used in the RegCM simulations is shown in Fig. 1. It encompasses a large area including East Asia, most of India, and the Tibetan Plateau at a horizontal grid point spacing of 60 km. Compared to the standard RegCM, updated land surface types are used over East Asia as provided by the Institute of Botany, Chinese Academy of Sciences. The analysis, which is limited to the China region, includes maximum and minimum daily temperature, number of rainy days, number of heavy rain days, and tropical storm occurrence. Observations for the evaluation of the present–day climate simulation are obtained from 160 observing stations distributed throughout China. In order to compare with observations, RCM simulated fields are linearly interpolated onto station locations.

## 3. Results

A basic analysis of the simulations discussed here is contained in Gao et al. (2001). They showed that the RegCM control simulation exhibited a general cold bias of a few degrees over extended regions of China mostly as a result of a corresponding cold bias in the CSIRO simulation. Concerning precipitation, the RegCM simulation showed a small overestimation of summer monsoon precipitation over south China, but the annual precipitation biases were

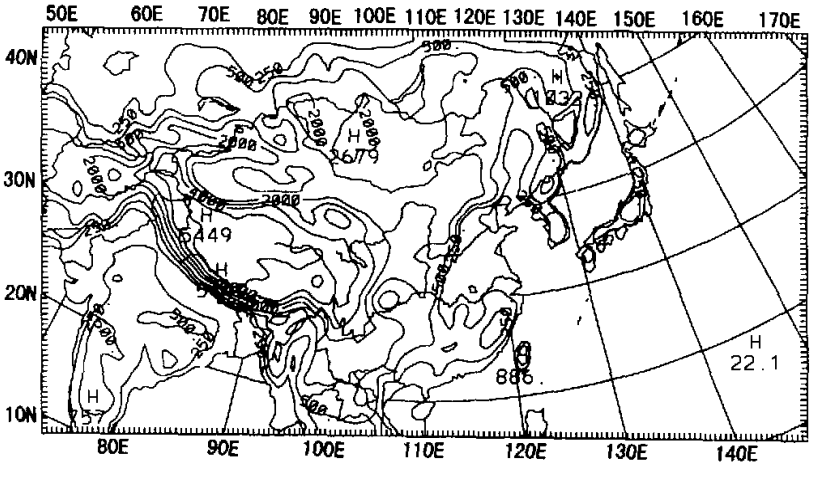


Fig. 1. Domain and elevation (units: m) in the RegCM / China.

generally small. The RegCM also improved the simulation of spatial structure of temperature and precipitation compared to the CSIRO model. The spatial correlation coefficient between simulated and observed annual temperature increased from 0.83 in the CSIRO to 0.92 in the RegCM and for annual precipitation from 0.48 in the CSIRO to 0.65 in RegCM. A similar improvement in the RegCM compared to CSIRO was found in all simulated months.

The $2\times CO_2$–control difference in annual average surface air temperature simulates a warming ranging from 2.2°C in south China to 2.8°C in north China. The simulated precipitation increases over most of China by a few percent to about 20% in $2\times CO_2$ conditions compared with the control run. The largest precipitation increase occurs over central–north China. Areas of precipitation decrease can be found over the northeast China coastal regions (up to −10%) and a small region in south China.

### 3.1 *Daily maximum and minimum temperature* ($T_{max}$ and $T_{min}$)

As an example of model performance in simulating surface temperature, Fig. 2 shows the observed and simulated annually averaged $T_{max}$ over China. The model reproduces the observed spatial structure of $T_{max}$, with a correlation of 0.88 between observed and simulated patterns. The magnitude of $T_{max}$ is well simulated in southeast China, however, a cold bias of 3–5°C is found in some other regions. As analyzed before, this bias is at least partially due to a corresponding bias in the CSIRO forcing field. It should also be noted that observing stations tend to be located in relatively low elevations and valley sites, which tend to overestimate the spatially averaged observed temperature. This can also artificially enhance the estimated model cold bias in mountainous regions. Daily minimum temperatures showed biases similar to those of Fig. 2, with a correlation coefficient of 0.92 between observed and simulated $T_{min}$. Thus it should be noticed that the results for $T_{max}$ and $T_{min}$ in north China might be not so solid as in south China.

Figure 3 shows the regional mean $2\times CO_2$–control difference in $T_{max}$ and $T_{min}$ for each month averaged over the China region. Also shown is the corresponding change in diurnal temperature range (Fig. 4). It can be seen that an increase in both $T_{max}$ and $T_{min}$ of the order of 0.5 to 4°C is simulated in all months except November, when a small decrease in $T_{max}$ is found. The temperature changes in Fig. 3 are statistically significant at the 90% confidence level in January and June for $T_{max}$ and in January, March, June, July, and August for $T_{min}$. It is evident from Fig. 3 that the increase of $T_{max}$ is lower than that of $T_{min}$ in most months, which causes a decrease in diurnal temperature range of a few tenths to 1°C. When annually averaged, the mean changes over China are about 1.6°C and 2°C for $T_{max}$ and $T_{min}$, respectively.

The annual mean change of $T_{max}$ and $T_{min}$ over China is shown in Fig. 5, in which station locations are indicated where the changes are statistically significant at the 90% confidence level. The increase in $T_{max}$ is most significant over southeast China, for example over the Zhejiang, Anhui, and Fujian provinces, with an average increase of 1.8°C. A larger number of station locations with statistically significant changes is found for $T_{min}$, especially over southeast and northeast China.

Of greater interest for the issue of extreme events is the change in $T_{max}$ during summer and $T_{min}$ during winter. These are shown in Fig. 6a and 6b, respectively, for the station locations. For the summertime $T_{max}$, the largest changes are found in the area ranging from southern part of Northeast China to northern part of Huabei, as well as the provinces of Shaanxi, Ningxia, and Gansu, which are mostly characterized by arid and semi–arid climates. The increase in winter $T_{min}$ is mostly significant over wide regions of central and southeast

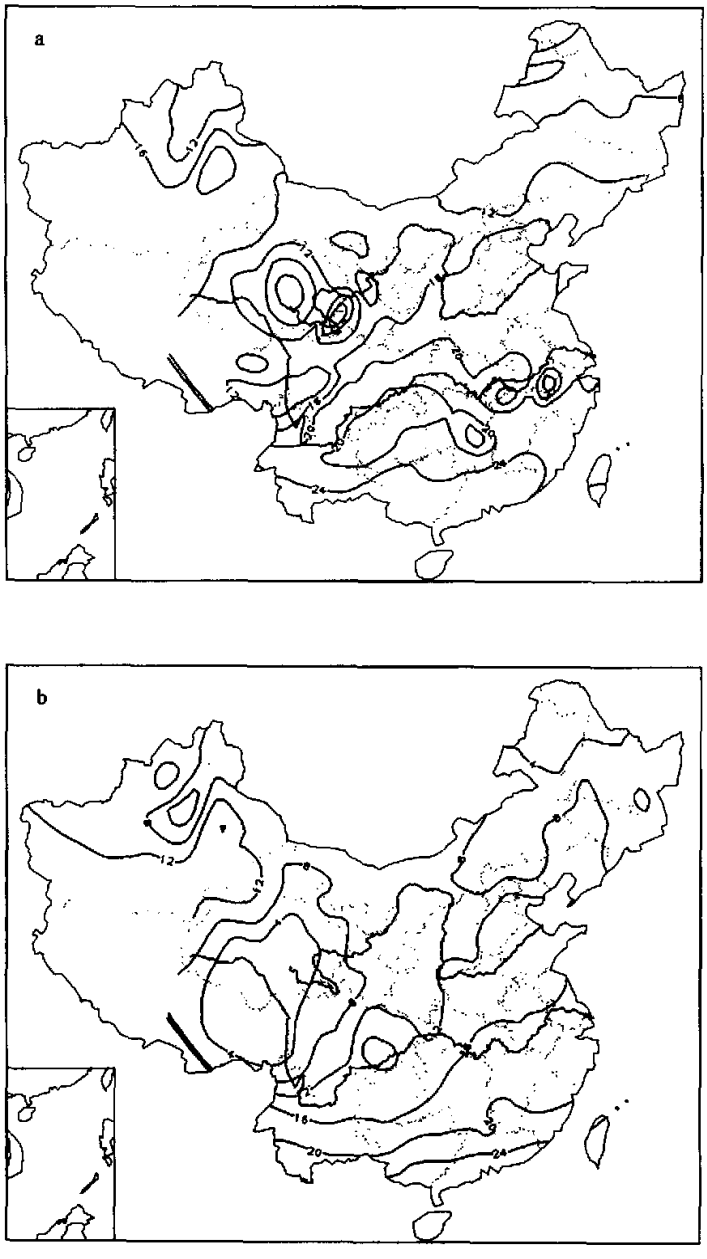


Fig. 2. Annual mean $T_{max}$. (a) observation, (b) simulation (units: °C) (correlation coefficient between the two: 0.88).

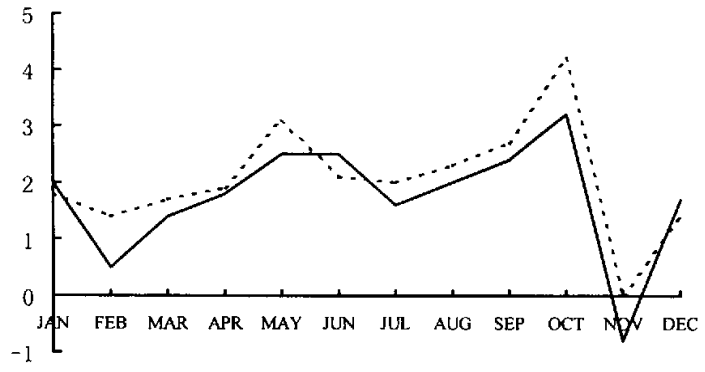


Fig. 3. Regional mean change of $T_{max}$ and $T_{min}$ over China due to GHG. The solid line is the change of $T_{max}$ and the dashed line is the change of $T_{min}$. Abscissa is month, ordinate is the change of temperature (units: °C).

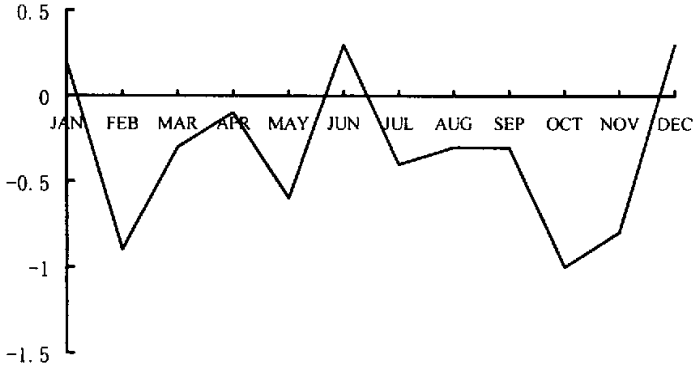


Fig. 4. Regional monthly mean change of diurnal temperature range over China due to GHG. Abscissa is month, ordinate is the change of dirunal temperature range (units: °C).

China (Fig. 6b).

Changes in summer $T_{max}$ and winter $T_{min}$ should produce corresponding changes in the occurrence of hot and cold spells. As an example, Table 1 shows the change in number of days with maximum temperature above 35°C in Beijing, in northeast China, and the change in number of days with minimum temperature below −10°C in Shangai, in central–east China. It can be seen that the change in hot spell days in Beijing is more than doubled in $2 \times CO_2$ conditions, while the number of cold spell days in Shanghai is nearly halved. Both changes are statistically significant at the 90% confidence level.

Summarizing the results of this section, both $T_{max}$ and $T_{min}$ increase in $2 \times CO_2$ conditions, but because of a greater increase in $T_{min}$, the diurnal temperature range decreases, with the change being statistically significant at the 90% confidence level in several months. The

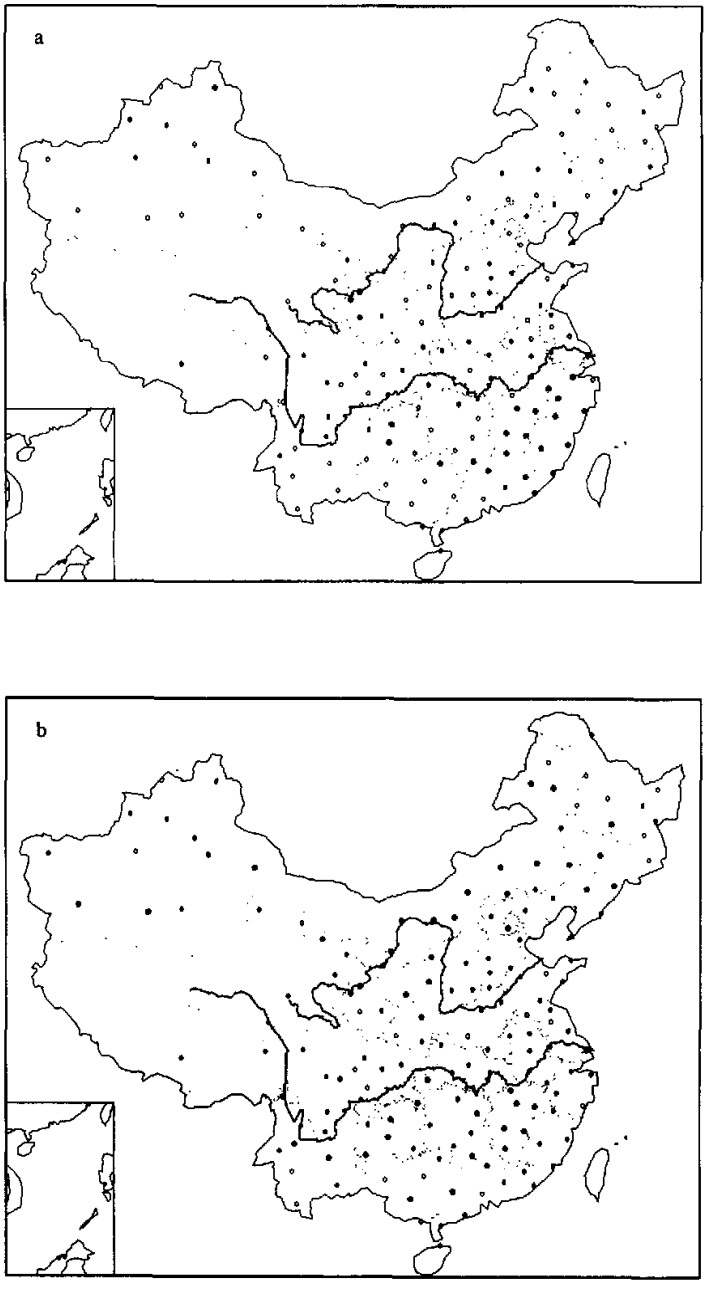


Fig. 5. Distributions of annual mean change of (a) $T_{max}$ and (b) $T_{min}$ in China with 0.10 significance due to GHG (●:0.6–2.4°C).

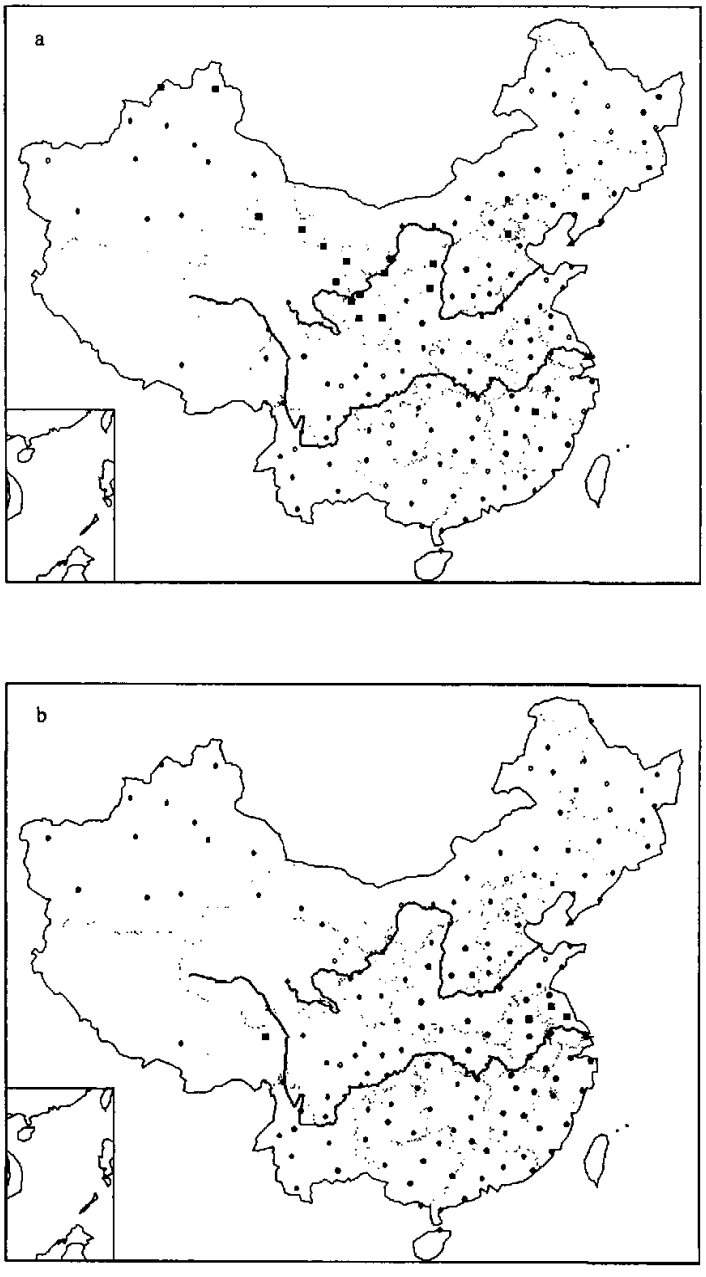


Fig. 6. Distributions of change for (a) $T_{max}$ in summer and (b) $T_{min}$ in winter over China with 0.10 significance due to GHG (●: 0.6–2.4°C ■: ≥ 2.5°C).

change shows regional variations, with the largest changes in annual average $T_{max}$ and $T_{min}$ occurring over southeast China and southeast and northeast China, respectively. Significant regional increases in summer $T_{max}$ and winter $T_{min}$ lead to corresponding substantial increases in hot spell days and decreases in cold spell days.

**Table 1.** Change of days for $T_{max}$ in summer in Beijing and $T_{min}$ in winter in Shanghai

| Beijing | | Shanghai | |
|---|---|---|---|
| Standard of $T_{max}$ (°C) | 35 | Standard of $T_{min}$ (°C) | −10 |
| Days of control run | 13 | Days of control run | 11 |
| Days of $2\times CO_2$ run | 27 | Days of $2\times CO_2$ run | 4 |
| Change (%) | 108 | Change (%) | −64 |

### 3.2 *Number of rainy days and heavy rain days*

Figure 7 shows the observed and control run annual average number of rainy days, defined here as days of precipitation in excess of 1 mm. The comparison shows that the model simulates well the number of rainy days, both in magnitude and spatial pattern. The number of rainy days is in excess of 160 over extended regions of southern China, while it is in the range of 40 to 80 over most of northeast and northwest China. The lowest number of rainy days is found in the Xinjiang province of northwest China. The pattern correlation between observed and simulated number of rainy days is 0.82.

Figure 8 shows the change in the number of rainy days for $2\times CO_2$ conditions at the station locations where this change is statistically significant at the 90% confidence level. It can be seen that the number of rainy days increases significantly only over regions of northeast and northwest China, where an increase in average precipitation was also simulated (Gao et al. 2001). Note that these are regions characterized by arid and semi-arid climate conditions. Over central and southeastern China, where precipitation is greater, the simulated changes in number of rainy days are not significant.

Figure 9 shows the observed and simulated number of days with heavy rain, defined here as daily precipitation in excess of 50 mm for the observations and 35 mm for the simulation. A lower threshold was selected for the simulation since the model precipitation is representative of the grid box average, while the observed precipitation is at the station location. With this scaling, the number of observed and simulated heavy rain events are of the same order of magnitude, from less than 1 day/year over northwest China to 4–6 days/year over southeast China. Most of the heavy rain episodes over China occur in correspondence with the summer monsoon, which sweeps from south China in May and June to central and northeast China in July and August. Although the broad scale pattern of heavy rain days in the simulation is consistent with the observations, the observed fine scale structure is not well reproduced by the model, with a pattern correlation coefficient of 0.50.

Change in the simulated number of heavy rain events is shown in Fig. 10, where the locations with a 90% confidence level of statistical significance are indicated. Significant changes mostly occur in South China, especially in the southeast area including the Fujian province and the western portion of the Jiangxi province. This area is affected by the monsoon front mostly in May and June. An additional center of increase in heavy rain events occurs in south of Guizhou and Sichuan provinces in southwest China. Isolated station locations in North China also show significant increases, while a significant decrease is indicated at only one station, where the average precipitation also decreases (see Gao et al. 2001). Overall, however,

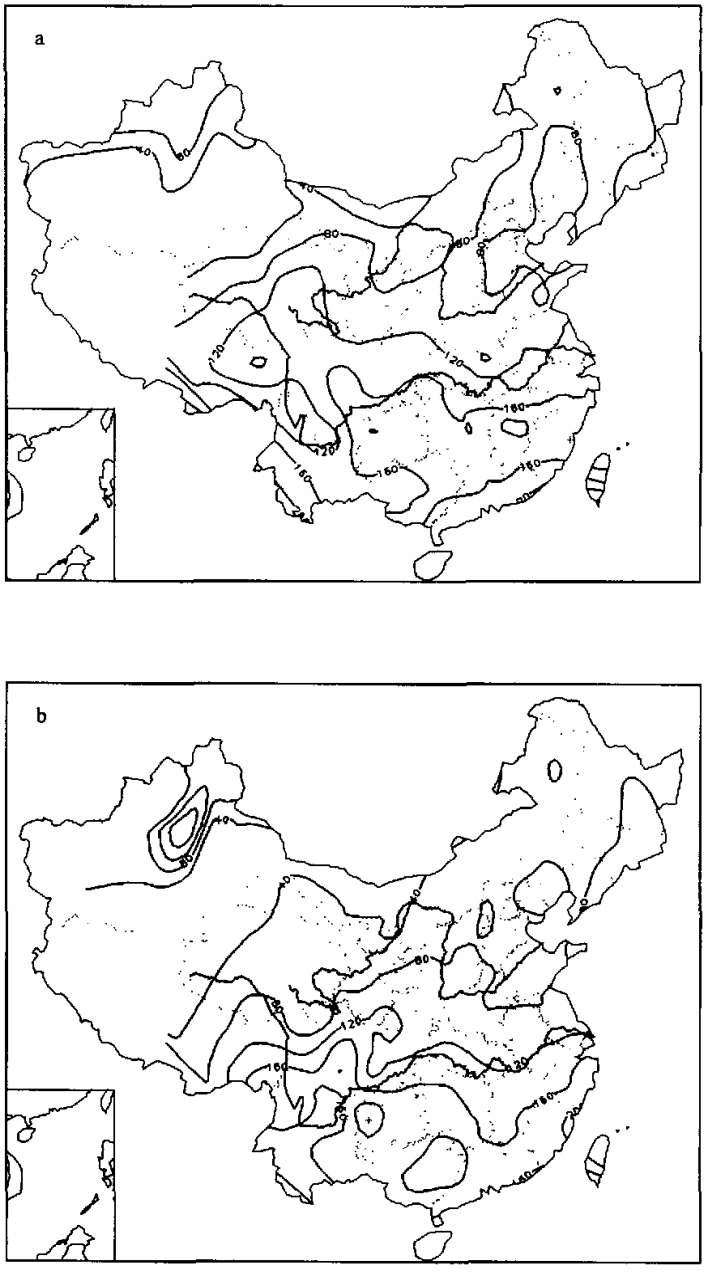


Fig. 7. Distribution of rainy days in China. (a) observation, (b) simulation (units: days / year) (correlation coefficient between the two: 0.82).

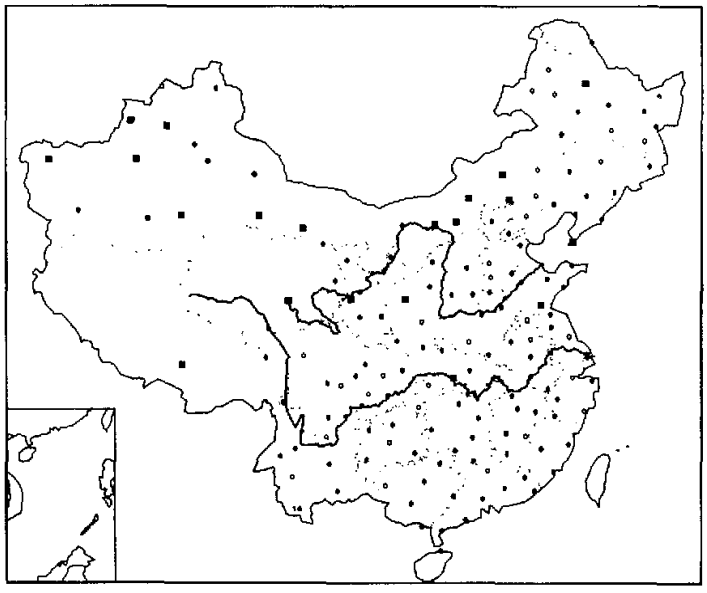

Fig. 8. Distribution of change of rainy days in China due to GHG (●: < 10 days / year ■: ≥ 10 days / year ▲: < −10 days / year).

Fig. 10 suggests a general increase in heavy precipitation events that is highly variable at the sub-regional scale.

### 3.3 *Tropical storms*

As mentioned, tropical storms and typhoons can have devastating impacts over China. East Asia typhoons move along two preferential routes, which we refer to as Route I and Route II. Route I includes typhoons that move westward across the western tropical Pacific and impinge upon central / east China; Route II typhoons move from south to north across the South China Sea towards the coastal regions of south China. On average about 4 tropical storms per year reach the mainland of China, and most tropical storm activity for the East Asia region takes place in July and August, therefore our analysis is limited to these two months.

In the regional model, a tropical storm is identified by a low sea level pressure (SLP) center of less than 1005 hPa of duration of at least three days during July and August. The threshold SLP is higher than that used in the Chinese Operational Weather Forecast Center (990 hPa) because the relatively coarse resolution of both regional and global models prevents simulation of very deep cyclones. Table 2 shows the number of landing typhoons (July and August only) in the control and $2 \times CO_2$ experiments, along with a partitioning into Route I and Route II typhoons.

In the control run, we find about 1.6 landing typhoons per year. Therefore, the model underestimates the number of typhoons over the region. This result is along the same lines as

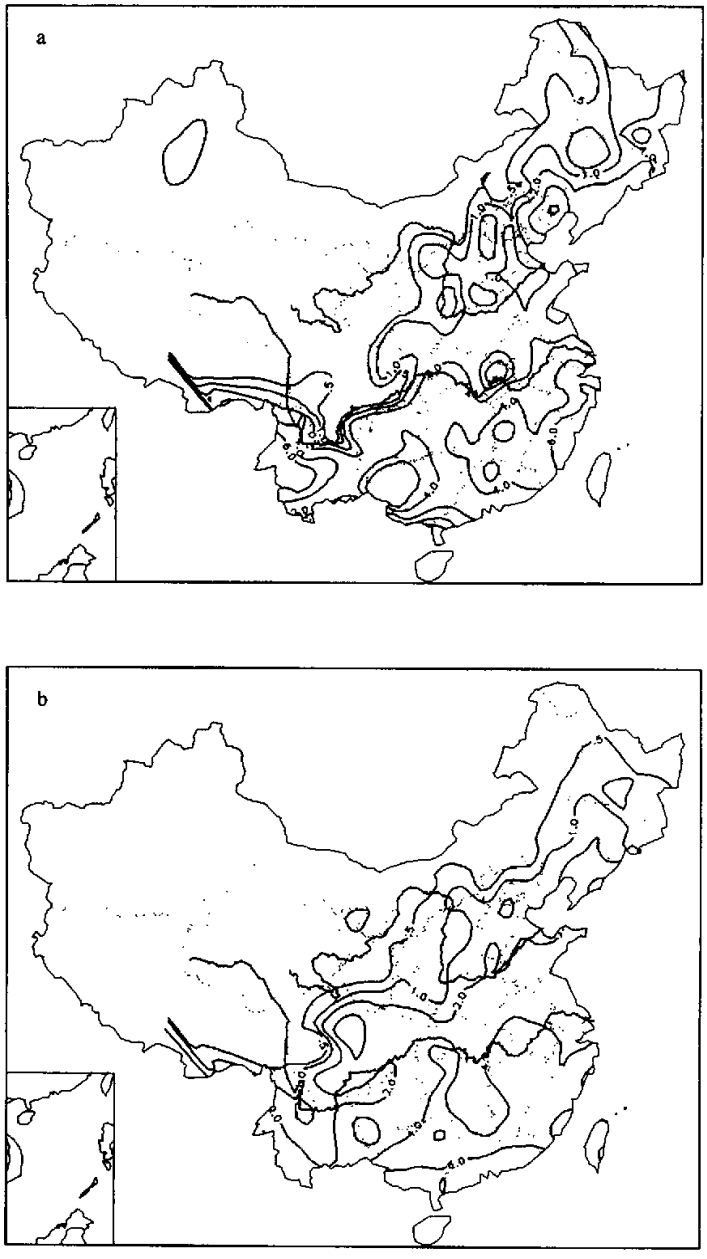


Fig. 9. Days of heavy rain in China. (a) observation, (b) simulation (units: days / year) (correlation coefficient between the two: 0.50).

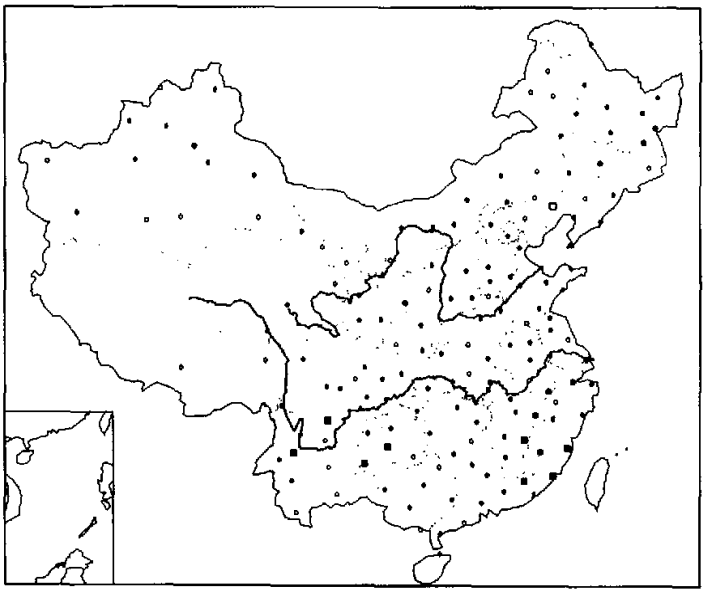

Fig. 10. Distribution of change of days of heavy rain in China with 0.10 significance due to GHG (●: < 3 dyas / year ■: ≥ 3 days / year □: < −3 days / year).

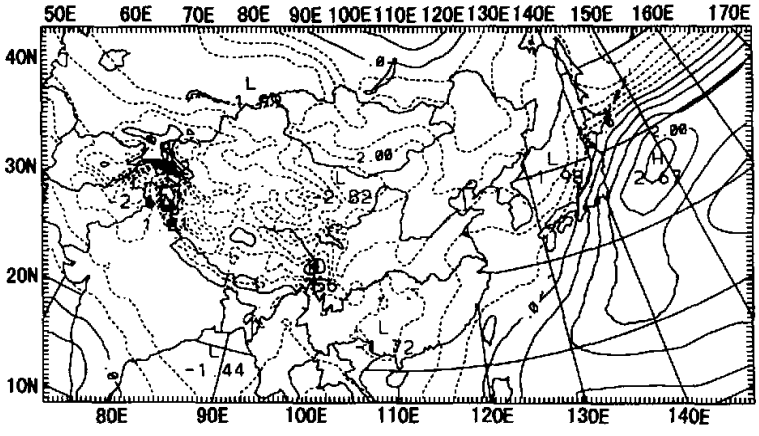


Fig. 11. SLP change in July and August (units: hPa).

**Table 2.** Simulated typhoons in July and August and their changes due to GHG

| | Control | GHG | Change (%) |
|---|---|---|---|
| Numbers of forming typhoons / year | 3.8 | 4.8 | +26 |
| Numbers (percentage) of forming typhoons following Route I | 2.4 (63%) | 1.6 (33%) | −33 |
| Numbers (percentage) of forming typhoons following Route II | 1.4 (37%) | 3.2 (67%) | +129 |
| Numbers of landing typhoons / year | 1.6 | 3.2 | +100 |

found by Hirakuchi and Giorgi (1995) in a previous nested regional climate simulation over the region, and thus points to a difficulty of models to simulate deep tropical cyclones, most likely due to resolution limitations in both the driving GCMs and the nested regional models. In $2 \times CO_2$ conditions, we find an increase of 26% in the number of forming typhoons, although this is not statistically significant at the 90% confidence level.

Table 2 shows that the characteristics of the typhoon route changes significantly in $2 \times CO_2$ conditions. While in the control run the largest fraction of typhoons (63%) follows Route I, in the $2 \times CO_2$ simulation about 67% of typhoons follow Route II. This leads to a substantial increase of landing typhoons over China. One of the reasons for this change can be understood by analyzing the simulated changes in July / August SLP (Fig. 11). It can be seen that in $2 \times CO_2$ conditions, the SLPs increase over the western Pacific to the east of China and decrease south of China. This SLP change pattern hinders the westward motion of typhoons along Route I, but enhances northward typhoon motion along Route II. This results in a greater number of tropical storms over south China and a lower number over central–east China.

## 4. Summary and conclusions

In this paper we analyze different measures of extreme events in present–day and $2 \times CO_2$ multi–year regional climate simulations over East Asia, with a focus on the China region. We find that both daily maximum and daily minimum temperature increase in $2 \times CO_2$ conditions, but the dirunal temperature range decreases due to the higher increase of minimum temperature. The number of hot spell days in summer significantly increases while the number of cold spell days in winter significantly decreases. The number of rainy days and heavy rain days increases over some sub–regions of China, most noticeably north China and southeast China. Tropical storms tend to increase and the dominant path of tropical storms landing over China shifts from westward across the tropical western Pacific to northward across the South China Sea.

The simulations analyzed here do not inlude the effects of aerosols, and are of relatively short duration (5 years) with the confidence test level being only 90%, so they should only be viewed as illustrative. However, they provide general indications along the lines of previous work on GHG–induced changes in extreme events (e.g., IPCC 2001). Longer experiments with more comprehensive forcing scenarios are needed for a more robust assessment of changes in extreme events due to increased GHG concentrations.

*Acknowledgments.* Thanks are due to CSIRO in Australia and the Institute of Botany, Chinese Academy of Sciences, National Climate Center of China, for providing the data sets of the GCM and the vegetation cover. This research was supported by the National Natural Science Foundation of China under Grant No. 40125014, National Key Programme for Developing Basic Sciences (G1998040900–part 1).

## REFERENCES


Dickinson, R. E., A. Henderson-Sellers, and P. J. Kennedy, 1993: Biosphere atmosphere transfer scheme (BATS) version 1e as coupled to the NCAR Community Climate Model, NCAR Tech. Note, NCAR / TN387+STR.

Durman, C. F., J. M. Gregory, D. H. Hassell, R. G. Jones, 2001: The comparison of extreme European daily precipitation simulated by a global and a regional climate model for present and future climates. *Quart. J. Roy. Meteor. Soc.*, **127**(573), 1005–1016.

Frei, C., C. Schar, D. Luthi, and H. C. Davies, 1998: Heavy precipitation processess in a warmer climate. *Geophys. Res. Lett.*, **25**, 1431–1434.

Gao, X. J., Z. -C. Zhao, Y. Ding, R. Huang, and F. Giorgi, 2001: Climate change due to greenhouse effects in China as simulated by a regional climate model. *Advances in Atmospheric Sciences*, **18**(6), 1224–1230.

Giorgi, F. M. R. Marinucci, and G. T. Bates, 1993a: Development of a second-generation regional climate model (RegCM2). Part I: Boundary-layer and radiative transfer processes. *Mon. Wea. Rev.*, **121**, 2794–2813.

Giorgi, F. M.R. Marinucci, G.T. Bates, and G. DeCanio, 1993b: Development of a second-generation regional climate model (RegCM2). Part II: Convective processes and assimilation of lateral boundary conditions. *Mon. Wea. Rev.*, **121**, 2814–2832.

Giorgi, F., C. S. Brodeur, and G. Bates, 1994: Regional climate change scenarios over the United States produced with a nested regional climate model. *J. Climate*, **7**, 375–399.

Giorgi, F., and Marinucci M. R., 1996: An investigation of the sensitivity of simulated precipitation to model resolution and its implications for climate studies. *Mon. Wea. Rev.*, **124**, 148–166.

Giorgi, F., L. Mearns, S. Shields, and L. McDaniel, 1998: Regional nested model simulations of present day and $2 \times CO_2$ climate over the Central Great Plains of the United States. *Climatic Change*, **40**, 457–493.

Giorgi, F., and C. Shields, 1999: Tests of precipitation parameterizations available in the latest version of the near regional climate model (RegCM) over the continental U.S. *J. Geophys. Res.*, **104**, 6353–6376.

Giorgi, F., and coauthors, 2001: Regional Climate Information-Evaluation and Projections. *Climate Change 2001*: The Scientific Basis, Contribution of WGI to the Third Assessment Report of IPCC, J. T. Houghton., Eds., Cambridge University Press, Cambridge, U.K., 583–638.

Gordon, H. B., and S. P. O'Farrell, 1997: Transient climate change in the CSIRO coupled model with dynamic sea ice. *Mon. Wea. Rev.*, **125**, 875–907.

Grell, G. A., 1993: Prognostic evaluation of assumptions used by cumulus parameterizations. *Mon. Wea. Rev.*, **121**, 764–787.

Hennessy, K. J., J. M. Greory, and J. F. B. Mitchell, 1997: Changes in daily precipitation under enhanced greenhouse conditions. *Clim. Dyn.*, **13**, 667–680.

Hirakuchi, H., and F. Giorgi, 1995: Multi-year present-day and $2 \times CO_2$ simulations of monsoon-dominated climate over eastern Asia and Japan with a regional climate model nested in a general circulation model. *J. Geophys. Res.*, **100**, 21,105–21,126.

Holtslag, A. A. M., E.I.F. Debruijin, H. L. Pan, 1990: A high resolution air mass transformation model for short-range weather forecasting. *Mon. Wea. Rev.*, **118**, 1561–1575.

IPCC, Climate Change 2001: The Scientific Basis, Summary for Policymakers and Technical Summary of WGI Third Assessment Report, eds. by J. T. Houghton, Y. Ding, et al., Cambridge University Press, Cambridge, UK, 72pp.

Kiehl, J. T., J.J. Hack, G.B. Bonan, B.A. Boville, B.P. Briegleb, D.L. Williamson and P.J. Rasch (1996): Description of the NCAR Community Climate Model (CCM3). NCAR / TN-420+STR.

Mearns, L. O., Bogardi, I., Giorgi, F., Matayasovszky, I., Palecki, M., 1999: Comparison of climate change scenarios generated daily temperature and precipitation from regional climate model experiments and statistical downscaling. *J. Geophys. Res.*, **104**, 6603–6621.

Mearns, L. O., and coauthors, 2001: Climate Scenario Development. *Climate Change 2001*: The Scientific Basis, Contribution of WGI to the Third Assessment Report of the IPCC, J. T. Houghton et al., Eds., Cambridge

University Press, Cambridge, U.K., 739–768.

Schar, C., C. Frei, D. Luthi, and H. C. Davies, 1996: Surrogate climate change scenarios for regional climate models. *Geophys. Res. Lett.*, **23**, 669–672.

# 东亚区域极端气候事件变化的数值模拟试验

高学杰 赵宗慈 Filippo Giorgi

**摘 要**

使用 RegCM2 区域气候模式，嵌套澳大利亚 CSIRO R21L9 全球海气耦合模式，进行了温室效应(二氧化碳加倍)对东亚(主要是中国区域)极端气候事件影响的数值试验。控制试验的结果表明，区域模式能够较好地模拟中国区域的极端气候事件。对温室效应引起的它们的变化进行了信度检验，分析结果表明，温室效应将引起日最高和最低气温增加，日较差减小；使得高温天气增多，低温日数减少。降水日数和大雨日数在一些地区将增加。同时还会引起影响中国的台风活动的变化。

**关键词**：区域气候模式，温室效应，极端气候事件